coatings

MDPI

Article

Defect-Free Large-Area (25 cm^2) Light Absorbing Perovskite Thin Films Made by Spray Coating

Mehran Habibi, Amin Rahimzadeh, Inas Bennouna and Morteza Eslamian *

University of Michigan-Shanghai Jiao Tong University Joint Institute, Shanghai 200240, China; mhabibi82@sjtu.edu.cn (M.H.); amin.rahimzadeh@sjtu.edu.cn (A.R.); inas.bennouna@etu.univ-nantes.fr (I.B.)

* Correspondence: Morteza.Eslamian@sjtu.edu.cn or Morteza.Eslamian@gmail.com; Tel.: +86-213-420-7249; Fax: +86-213-420-6525

Academic Editor: Alessandro Lavacchi

Received: 20 January 2017; Accepted: 9 March 2017; Published: 12 March 2017

Abstract: In this work, we report on reproducible fabrication of defect-free large-area mixed halide perovskite ($CH_3NH_3PbI_{3-x}Cl_x$) thin films by scalable spray coating with the area of 25 cm^2. This is essential for the commercialization of the perovskite solar cell technology. Using an automated spray coater, the film thickness and roughness were optimized by controlling the solution concentration and substrate temperature. For the first time, the surface tension, contact angle, and viscosity of mixed halide perovskite dissolved in dimethylformamide (DMF) are reported as a function of the solution concentration. A low perovskite solution concentration of 10% was selected as an acceptable value to avoid crystallization dewetting. The determined optimum substrate temperature of 150 °C, followed by annealing at 100 °C render the highest perovskite precursor conversion, as well as the highest possible droplet spreading, desired to achieve a continuous thin film. The number of spray passes was also tuned to achieve a fully-covered film, for the condition of the spray nozzle used in this work. This work demonstrates that applying the optimum substrate temperature decreases the standard deviation of the film thickness and roughness, leading to an increase in the quality and reproducibility of the large-area spray-on films. The optimum perovskite solution concentration and the substrate temperature are universally applicable to other spray coating systems.

Keywords: mixed halide perovskite; large area perovskite; spray coating; perovskite solution physical properties; perovskite film optimization

1. Introduction

Within the past few years, a tremendous effort has been made to increase the power conversion efficiency (PCE) of perovskite solar cells (PSCs). In spite of achieving remarkable PCEs in the research labs, as high as 22.1% [1], two main obstacles still hinder the development of this technology: The device instability and the lack of knowledge and experience for large scale and large area device fabrication. Development of commercial methods for the fabrication of large area PSCs is one of the prerequisites for their commercialization, and it is as important as stabilizing the PSC performance. It is generally expected that, by increasing the film surface area, the defect and pinhole density would increase; therefore, research on the development of large area solar cells is essential. An ideal perovskite film must have a fully-covered monocrystalline structure with high uniformity and low roughness. Obtaining such ideal films is challenging if not impossible, due to the special behavior of the halide perovskite materials, which is the tendency to crystallize in a polycrystalline structure upon deposition, making the resulting thin films prone to dewetting due to crystallization (crystallization dewetting), and, therefore, the emergence of pinholes [2]. Perovskite crystal growth in all directions, including the direction normal to the film, tends to shrink and disintegrate the film, resulting in a decrease in the film coverage and an increase in the roughness. An ideal perovskite film must have a thickness

within the range suitable for charge generation and transfer, as well. Thickness of the mixed halide perovskite films should be limited to 1 μm or so, dictated by the maximum diffusion length of the generated excitons in the perovskite structure [3]. Therefore, controlling the detrimental effect of the crystallization dewetting to achieve a fully-covered film, which also has desirable thickness and low roughness is quite challenging, especially when the film is deposited by a scalable method.

Solution-processed deposition of a thin film of perovskites may be performed using various casting methods, such as spin coating, dip-coating, doctor blading, spray coating, inkjet printing, screen printing, drop casting, slot-die coating, etc. Some of the aforementioned techniques, such as spin coating, in spite of providing precise controllability on the film morphology (thickness, coverage and roughness), are generally limited to batch processes and/or thin films with small effective surface areas, making them unsuitable for real-world applications. In the lab-scale and mostly using spin coating, various treatments are usually applied on the small-area perovskite films to reduce the roughness and increase the coverage and homogeneity and improve the crystalline structure. These methods include but are not limited to solvent engineering [4–6], manipulating the stoichiometry of the perovskite precursors (e.g., ratio of PbI_2/MAI solutions, where MAI stands for methylammonium iodide) [7,8], introducing additives to the perovskite solution (e.g., water, 1,8-diiodooctane(DIO)) [9,10], and controlling the annealing temperature and time [11]. However, preparation of large area perovskite films (>1 cm^2) with uniform characteristics across the film is harder to accomplish, compared with the films with small areas ($\leq$0.1 cm^2). Enlarging the perovskite surface area causes a decline in the cell performance. Figure 1 compares the PCE of several PSCs made under identical conditions, but using various deposition methods and effective surface areas. The figure confirms a systematic drop in the PCE after enlarging the active area of similar cells, or as a result of module fabrication by connecting various small-area cells in series, in order to increase the effective area [7,12–14].

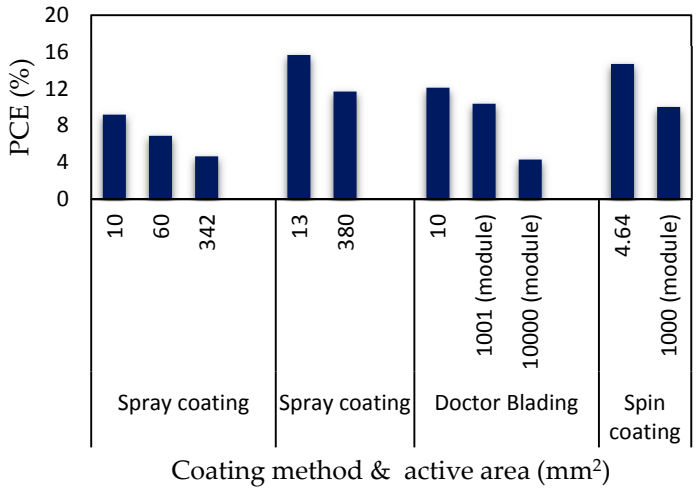

Figure 1. Degradation in the PCE of the PSCs made by various deposition techniques after enlarging the active area of individual cells, or by fabricating modules through connecting several small-area cells in series (data were taken from Refs. [7,12–14]). The precursor solutions associated with the mentioned coating processes are $MAPbI_3$, $MA(I_xBr_{1-x})_3$, PbI_2, and $MAPbI_3$, respectivley, and from left to right. In the doctor blading case, the perovskite layer was obtained by dip coating of the blade-coated PbI_2 film in the methylamonium iodide solution [12].

Following the aforementioned argument regarding the need for the fabrication of large-area solar cells using scalable methods, in this work, spray coating is used to produce large-area perovskite thin films with favorable morphological and light absorbing characteristics. This work focuses on the optimization of the perovskite light harvester layer only, and the fabrication of the entire device with large area is postponed to future works. Several advantages of spray coating compared to the other large scale casting techniques including the touch-free, low-cost and fast process, the possibility

for deposition on flexible or rough substrates, and its capability for producing ultrathin films, assure its high potential for the roll-to-roll fabrication of solar cells on a large scale [7,15]. Spray coating may be also combined with shadow masks for pattern printing. Recently, it has been reported that spray-on films show better thermal stability compared to spun-on films [16]. Huang et al. [16] demonstrated that the prolonged annealing time required after spin coating may adversely affect the stability of spun-on films, whereas the spray-on perovskite films show high thermal stability, which originates from better crystallinity of spray-on perovskite films. In their study, they also observed better optoelectronic characteristics in spray-on perovskite films compared to spun-on counterparts, due to their higher carrier lifetime and better charge transfer capability. Despite the advantages of spray coating, fabrication of fully-covered and homogeneous thin (perovskite) films with desired low thickness and roughness is challenging. This is because the phenomenon of the liquid atomization and spraying is a random and stochastic process, which works based on transient impact of numerous droplets of different sizes across the wetted area. The droplets may first form a stable or unstable thin liquid film and then dry to form a thin solid film, or each individual droplet or patch of several merged droplets may dry to form a thin solid film. These uncertainties may cause unpredicted characteristics in the ensuing thin solid films [17]. The photovoltaic characteristics of a solar cell, such as its open-circuit voltage (V_{OC}) and fill factor (FF), are directly influenced by the quality of the film. Voids and pinholes in the perovskite films caused by a poor spray coating process may make short circuit pathways between the above and underneath layers of the perovskite, which may result in a decrease in the device shunt resistance and degradation of the device performance. Therefore, some pre-treatments, post-treatments, or additional processes have been suggested to achieve a desired spray-on thin film. For instance, Ramesh et al. [7] used a simple airbrush pen to spray $CH_3NH_3PbI_3$ perovskite precursor solution and tuned the ratio of the MAI to PbI_2 precursor solutions, spray flow rate, substrate temperature, and annealing temperature to achieve a desired film. In another work, Chandrasekhar et al. used electrostatic spray coating to spray the MAI solution onto a pre-cast PbI_2 film, where a more uniform and dense perovskite film with lager crystals was obtained, compared to that of the conventional spray coating [18]. Heo and coworkers [19] synthesized $CH_3NH_3PbI_{3-x}Cl_x$ powder and then dissolved it in a mixture of DMF (dimethylformamide) and GBL (g-butyrolactone). To adjust the perovskite crystal size in the spray-on film, they controlled the evaporation rate of DMF by changing the ratio GBL to DMF. Abdollahi Nejand et al. [20] sprayed a concentrated solution of $CH_3NH_3PbI_{3-x}Cl_x$, which caused the creation of columnar film of perovskite. Then, the film was exposed to low-pressure vapor of DMF to partially dissolve the crystals; the weakened film was then compacted by a cold-roll press. Through this method, the film coverage and the device performance were improved. Concurrent spraying of perovskite precursors using two spray nozzles is another suggested technique to control the film composition and achieve a pinhole-free film of perovskite [14]. In the literature, spraying of the MAI solution over a pre-cast PbI_2 film in a sequential deposition has been reported, as well [8,18,21–23]. Zabihi et al. sprayed perovskite precursor solutions sequentially, using two spray nozzles, on an ultrasonically vibrating substrate to form a mixed halide perovskite film [22]. The substrate vibration resulted in improved mixing and uniform deposition of the perovskite layer. In a recent work, we also used spray coating in a perovskite solar cell to fabricate a uniform PbI_2 layer and then converted it to single-halide $MAPbI_3$ perovskite film via pulsed-spray coating and drop casting of the MAI solution atop the PbI_2 layer [23].

Although spray deposition of a uniform and pinhole-free film of mixed halide perovskites (e.g., $CH_3NH_3PbI_{3-x}Cl_x$) in a PSC with planar structure is challenging, the mixed halide perovskites are more advantageous over single halide perovskites, e.g., $CH_3NH_3PbI_3$, due to larger charge carrier diffusion lengths (near 10 times), which results in a higher charge collection efficiency [19]. Therefore, in this work, single-step spray deposition of the mixed halide perovskite $CH_3NH_3PbI_{3-x}Cl_x$ is adopted. Then, the morphological and optoelectronic characteristics of the fabricated perovskite films with a square area of 25 cm^2 are optimized by systematically tuning the important process parameters, i.e., the solution concentration, substrate temperature, and the number of spray passes, while other parameters

are pre-optimized and kept constant during the experiments. The best concentration of the solution of $CH_3NH_3PbI_{3-x}Cl_x$ dissolved in DMF is determined based on measuring the physical characteristics of the perovskite solution and also considering the detrimental effect of the crystallization dewetting that occurs at high solution concentrations [2]. The surface tension, contact angle and viscosity of the perovskite precursor solution are the main physical properties that govern the droplet impact and the coating process, and therefore are measured and reported in this work. The second important parameter, which is controlled to achieve a fully-covered film, is the substrate temperature. To begin with, a reasonable range of high temperatures is chosen due to the better spreading of droplets on high substrate temperatures (deduced by the measured contact angles versus temperature), and then the best substrate temperature is found based on the conversion of precursors to perovskite. Finally, the number of spray passes is tuned to achieve a fully-covered film with the lowest roughness and desired thickness. Standard deviation of the roughness and thickness data obtained from the spray-on films fabricated on a hotplate are lower than their counterparts sprayed on substrates kept at the ambient temperature. This fact reveals the strong feature of the high substrate temperature to increase the reproducibility of the spray-on films. It is important to distinguish between the substrate temperature in spray coating and the long-duration annealing temperature performed after the deposition process. In this work, all deposited samples were annealed on a hotplate at 100 °C for two hours.

2. Experimental

2.1. Materials and Methods

Lead chloride ($PbCl_2$, 98.5%), and N,Ndimethylformamide (DMF, 99.8%) were supplied by Sigma-Aldrich, St. Louis, MO, USA. Methylammonium iodide (MAI, 99.5%) was purchased from Xi'an Polymer Light Technology Corp. (Xi'an, China). MAI and $PbCl_2$ were mixed in 3:1 molar ratio and then dissolved in DMF in various concentrations (5% to 50% weight ratio: Ratio of the solid precursors mass to the total mass of the solvent and solid precursors in the solution). The $MAPbI_{3-x}Cl_x$ solution was heated to 60 °C and stirred on a magnetic stirrer overnight, and then cooled at room temperature. Small (1 × 1 cm^2) and large (6 × 6 cm^2) fluorine-doped tin oxide (FTO)-coated glass substrates with an average roughness of near 14.5 nm were cleaned by a mixture of deionized water and soap, acetone and isopropyl alcohol in an ultrasonic bath, sequentially. Then, the substrates were exposed to UV-Ozone irradiation for 15 min. Spray coating was performed by replacing the spray nozzle of an automatic spray coating system (Holmarc, Opto-Mechatronics Pvt. Ltd., Model HO-TH-04, Kochi, India) with a low flow rate commercial airbrush pen. This was done because the liquid container of the original ultrasonic nozzle of the Holmarc machine is excessively large, resulting in the wastage of the perovskite solution. The installed airbrush generates a fine mist, is easy to control, and is suitable for the fabrication of perovskite films. The speed and position of the spray nozzle in the x–y plane were controlled by software to move the nozzle in a continuous and raster movement to simulate an industrial spray coating process. The perovskite solution was atomized by the pressurized air at constant pressure and air flow rate. Parameters of the spray coating process are summarized in Table 1. Pictures of the spray coating machine and the spray nozzle are shown in Figure 2.

Table 1. Spray coating parameters for the fabrication of perovskite films.

Spray Parameters	Value
Nozzle to substrate distance (cm)	12
Nozzle speed (mm/s)	150
Flow rate (μL/s)	15
Air pressure (bar)	3.5
Number of passes	40, 70, 100
Substrate temperature (°C)	25–200

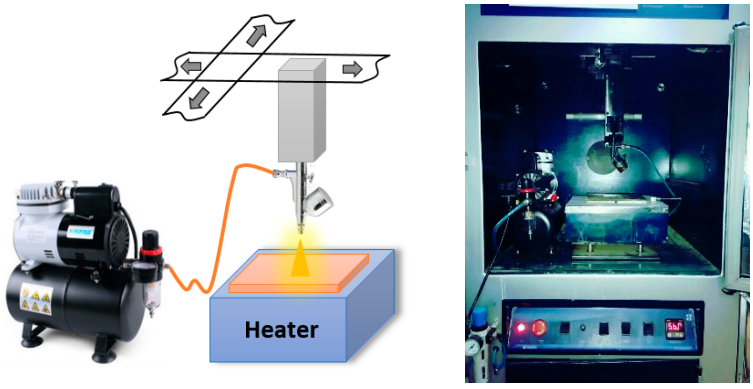

(**a**) (**b**)

Figure 2. (**a**) schematic of the spray coating process and the aparatus. (**b**) picture of the Holmarc spray coating system, which accomodates the spray nozzle and the hotplate shown in (**a**).

The relative humidity of Shanghai during the spray deposition of the perovskite films was in the range of 35% to 50% in different days. Although the humidity has a detrimental effect on the perovskite quality, it mainly affects the perovskite film during and after annealing. Therefore, to minimize the effect of the humidity, the spray-on films, made in the ambient conditions in few minutes, were transferred to the glovebox after deposition and initial drying on the high temperature substrate, for complete drying and annealing on a hotplate at 100 °C, for two hours. In some of the tests (for determination of the crystallization dewetting), the samples were formed on small-size FTO-coated glass (1 × 1 cm^2) by spin coating at 2500 rpm for 20 s, and then the samples were annealed based on the same procedure mentioned above for the spray-on films. Perovskite films made on small area FTO-coated glass were encapsulated with poly (methyl methacrylate) (PMMA) to enhance the perovskite stability against humidity during the X-ray diffraction (XRD) and absorption tests.

2.2. Film and Device Characterization

Optical microscopy images of perovskite films were taken by a confocal laser scanning microscope (CLSM 700, Carl Zeiss AG, Oberkochen, Germany) and scanning electron microscopy (SEM) images were obtained using a Hitachi microscope, Model S-3400N, Tokyo, Japan. Average thickness and roughness of the films were measured by a stylus profilometer (KLA-Tencor P7, Milpitas, CA, USA). Roughness values were measured and averaged along six randomly chosen lines of 100 µm long, on two similar samples, in each case. Thickness values were also measured by the same instrument, in four randomly-chosen spots near the edge of the films with respect to the uncovered areas of the FTO-coated glass, and were averaged.

The conversion of the MAI and $PbCl_2$ precursors to mixed halide perovskite and the absorption of the perovskite films were evaluated by X-ray diffraction (XRD, model D5005, Bruker, Billerica, MA, USA) and UV-Visible absorption spectrophotometry (EV300, Thermo Fisher Scientific, Waltham, MA, USA), respectively. Physical properties of the perovskite solutions were measured, as well. The solution surface tension and contact angle were measured, using Theta Lite Optical Tensiometer (Biolin Scientific AB, Gothenburg, Sweden), and the viscosity was measured using a digital rotary viscometer (model NDJ-8S, Jiangsu Zhengji Instruments Co., Ltd., Jintan, China) in various concentrations, defined as the weight fraction of the solute (perovskite precursors) in the solution. A digital infrared camera (FLIR C2, Tallinn, Estonia) was used to confirm the substrate temperature, which is generated and maintained by an electric heater.

3. Results and Discussion

Knowledge of the concentration-dependent physical properties of the perovskite precursor solution, such as the contact angle, surface tension, and viscosity, would lead to better understanding of the droplet impact behavior during spray deposition, and also would help proper selection of the solution concentration. This is because the droplet impact dynamics is governed by the Ohnesorge number, a dimensionless group based on the liquid properties, as well as Reynolds and Weber numbers, which include the effect of the droplet momentum upon impact. Assuming constant impingement velocity and substrate texture and surface energy, concentration of the perovskite precursor solution and the substrate temperature control the spreading behavior of the perovskite droplets after impinging on the substrate, and therefore control the morphology of the resulting perovskite film. Physical properties of the precursor solution may also affect the thin film characteristics prepared by other casting methods. Various solution concentrations (9.5–33 wt.%) [20,24,25] have been used by others as the starting concentration for the fabrication of perovskite films, but, to the best of our knowledge, this has not been done systematically. Therefore, here we measured the contact angle, surface tension and viscosity of the mixed halide perovskite $MAPbI_{3-x}Cl_x$ dissolved in DMF solvent in a wide range of concentrations (5–50 wt.%). Table 2 lists the average measured properties along with the standard deviation of the measurements.

Table 2. Some of the physical properties of mixed halide perovskite solution ($MAPbI_{3-x}Cl_x$ in DMF) at various concentrations (wt.% of solute in the solution). MAI and $PbCl_2$ powders were mixed in 3:1 molar ratio and then dissolved in DMF to achieve various concentrations.

Concentration (wt.%)	Viscosity (mPa.s)	Surface Tension (mN/m)	Contact Angle (°)
0	0.887 ± 0.02	37.29 ± 0.02	12.39 ± 0.04
5	1.0 ± 0.0	36.81 ± 0.02	16.35 ± 0.24
10	1.0 ± 0.0	35.18 ± 0.02	20.79 ± 0.10
20	1.59 ± 0.016	34.39 ± 0.06	24.00 ±0.15
30	2.0 ± 0.0	31.44 ± 0.03	29.26 ± 0.11
40	2.0 ± 0.0	29.80 ± 0.03	30.40 ± 0.15
50	6.72 ± 0.135	28.87 ± 0.02	31.65 ± 0.21

Some studies, e.g., Mullins and Sekerka [26], suggest that some ionic solutions may act like a surfactant, in that, their surface tension may decrease with the solution concentration, and, in fact, our data of perovskite solutions at different concentrations comply with the reported observations for other similar solutions. Figure 3a shows a decrease in the surface tension of the perovskite solution with the solution concentration. On the other hand, examination of the perovskite solution droplets on glass substrates shows that the contact angle increases with concentration (Figure 3b). Young's equation, i.e., $\gamma\cos\theta = \gamma_{sg} - \gamma_{ls}$, relates the binary surface tensions with the equilibrium contact angle on a solid surface. In Young's equation, γ is the liquid–air surface tension or simply surface tension, γ_{sg} is the solid-gas surface tension, γ_{ls} is the liquid–solid surface tension, and θ is the equilibrium contact angle. Our results show that, as the solution concentration increases, γ decreases on one hand and contact angle increases on the other hand ($\cos\theta$ decreases), thus the solid–liquid surface tension, γ_{ls} must increase, since the solid–gas surface tension γ_{sg} remains constant for the same glass substrate next to the same surrounding gas (air). Some numerical works by Sear [27] and theoretical works by Djikaev and Ruckenstein [28] have shown the substrate effect on crystal nucleation. For instance, crystal nucleation is greater in the vicinity of the gas–liquid–solid triple line, since the concentration is the highest at the triple line, due to the coffee stain or coffee ring effect. Hence, to suppress the inhomogeneous crystal nucleation due to the coffee-ring effect, increasing the spreading of the solution droplets, as well as increasing the droplet drying rate, could be effective. In this work, this has been achieved by using treated FTO-coated glass substrates to increase wettability, as well as by choosing a low solution concentration (e.g., 10%), to achieve a low contact angle.

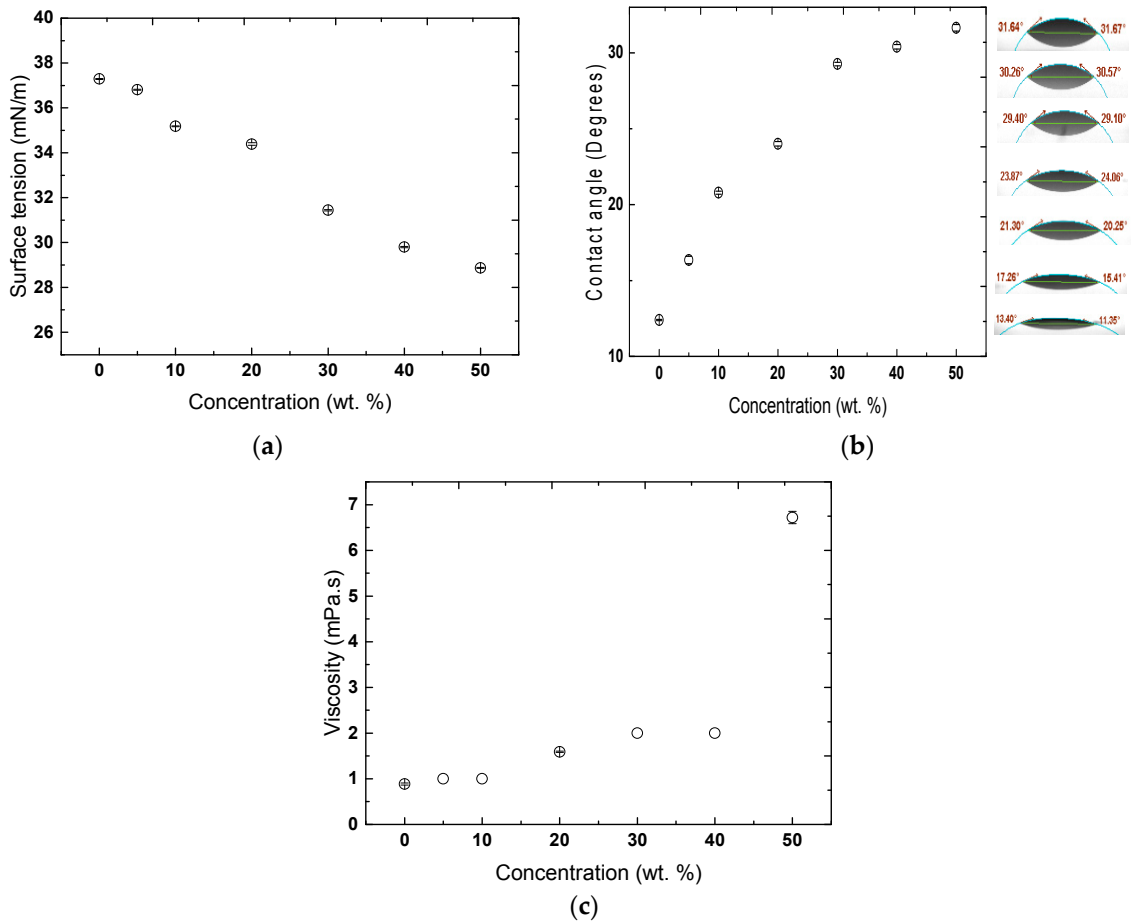

Figure 3. Variation of the physical properties of the mixed halide perovskite solution ($MAPbI_{3-x}Cl_x$ in DMF) versus solution concentration in wt.% of solute in solution. (**a**) liquid–air surface tension; (**b**) contact angle, and (**c**) viscosity. Note: The data and the associated errors are listed in Table 1.

Viscosity is another physical property of the liquid solution that affects the liquid film spreading and wetting, and is believed to increase nonlinearly as the solvent evaporates and the liquid film partially dries [29]. In droplet-based coating methods, viscosity, through the Ohnesorge number, affects droplet impact dynamics and spreading. As shown in Figure 3c, viscosity increases somewhat linearly at concentrations up to about 40 wt.%. Then, it sharply increases as the concentration increases to 50 wt.%, which corroborates the nonlinear behavior of the viscosity with the concentration. This is because, at high concentrations, the solution starts to show non-Newtonian behavior.

High concentration of the perovskite solution may cause the formation of larger crystals in the film and therefore surface dewetting, i.e., crystallization dewetting [2], which obviously leads to the formation of rough films with pinholes (Figure 4). All films in Figure 4 are spun under the same conditions, while the concentration changes from 10% to 30% and 50% from left to right, respectively. Since the data from Figure 3 clearly show that the solution droplets with lower concentration have smaller contact angles, and therefore higher surface wettability, and Figure 4 shows that smaller detrimental crystallization dewetting occurs when the perovskite thin films are made using a solution concentration of 10 wt.%, this concentration is selected as the favorable concentration for spray coating of the mixed halide perovskite $MAPbI_{3-x}Cl_x$ dissolved in DMF. At this low concentration, the crystallization dewetting is the minimum and spreading is the maximum, both favoring the formation of a continuous and defect-free film.

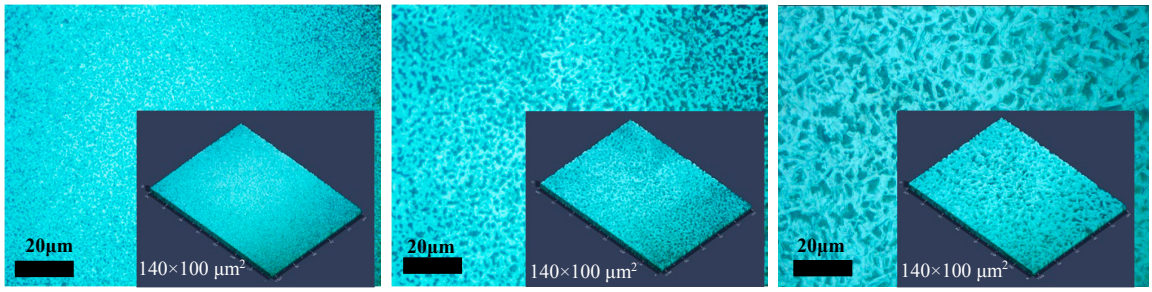

Figure 4. Optical images of spun-on perovskite films at different concentrations. The solution concentrations are (**a**) 10 wt.%; (**b**) 30 wt.%; and (**c**) 50 wt.%. This figure shows that high concentrations result in the formation of large crystals, and therefore, occurrence of crystallization dewetting.

Having determined the ideal solution concentration, now we will find the optimum substrate temperature. Spray deposition of perovskite solution on a low temperature substrate prolongs the drying time, which may adversely affect the film coverage [24]. This is due to the prolonged crystal growth at low temperatures and therefore the occurrence of crystallization dewetting. Figure 5 shows the range of the substrate temperatures (during the coating process) that have been used in recent published papers [3,7,8,13,16,18–22,24,25,30–37], in order to fabricate the perovskite layer of PSCs, mostly by a scalable technique. These techniques include spray coating, doctor blading, slot-die coating, roller coating, inkjet printing, and drop casting. In most of the methods, temperature of the substrate was raised to facilitate the coating process. However, in most of those works, a systematic procedure was not followed. Hence, in this work, the best substrate temperature for rapid drying and in situ heat treatment during spray deposition is selected based on two criteria; first, a range of temperatures are selected to achieve the best droplet spreading upon impingement on a hot substrate. To this end, the contact angles of 10 wt.% perovskite solution droplets were evaluated right after droplet release on glass substrates kept at various temperatures (25 °C to 200 °C with 25 °C intervals) (Figure 6a). The heated substrate increases the evaporation rate, which is beneficial for arresting the crystal growth and suppressing the crystallization dewetting. In addition, the data of Figure 6a show that a higher substrate temperature improves the film coverage by decreasing the contact angle, because of better droplet spreading and surface wettability. Therefore, based on the contact angle measurements, relatively high substrate temperatures seem to be more effective for a better coverage. It is noted that recent research on the thermal and thermodynamic stability of perovskites proves that high annealing temperatures for a long time results in the decomposition of the perovskite structure [38,39]; however, here in this work, the films are exposed to a high substrate temperature for a short period of time during the spray deposition, which lasts only for several seconds. It is also noted that excessive substrate temperatures above the Leidenfrost temperature must be avoided due to the formation of a vapor film over the substrate, which would interrupt the droplet spreading and the coating process.

In the second step, we further narrow down the choices of the substrate temperature by evaluating the conversion of the perovskite precursors to perovskite. We define the conversion ratio using the XRD patterns of the perovskite films, as the ratio of the PbI_2 peak intensity at 12.7° to the perovskite peak intensity at 14.2°. PbI_2 is an impurity in the perovskite film and has to be eliminated or minimized. Figure 6b illustrates the XRD patterns of four samples fabricated on substrates kept at 25, 100, 150 and 200 °C. It is noted that these are the substrate temperatures, and all samples were annealed at 100 °C after deposition. We observe that the intensity of the PbI_2 peak changes with the substrate temperature. Figure 6c shows the conversion ratio obtained at various substrate temperatures. It is observed that the maximum conversion occurs near 150 °C, which is near the boiling point of DMF, i.e., 153 °C. Low conversion ratio at temperatures lower than 150 °C is ascribed to initial incomplete conversion of precursors, whereas, at higher temperatures than the boiling point of DMF, it may be attributed

to rapid evaporation of the solvent and the lack of enough solvent for a complete conversion. This observation is in agreement with the report of Mallajosyula and coworkers that considered substrate temperature of 145 °C during doctor blading of $MAPbI_3$ [37]. Therefore, according to the contact angle measurements of perovskite droplets at various substrate temperatures and also the conversion ratio data, 150 °C is chosen as the optimum substrate temperature, since, at this temperature, spreading of perovskite solution droplets and also conversion ratio of perovskite attain their maximum values.

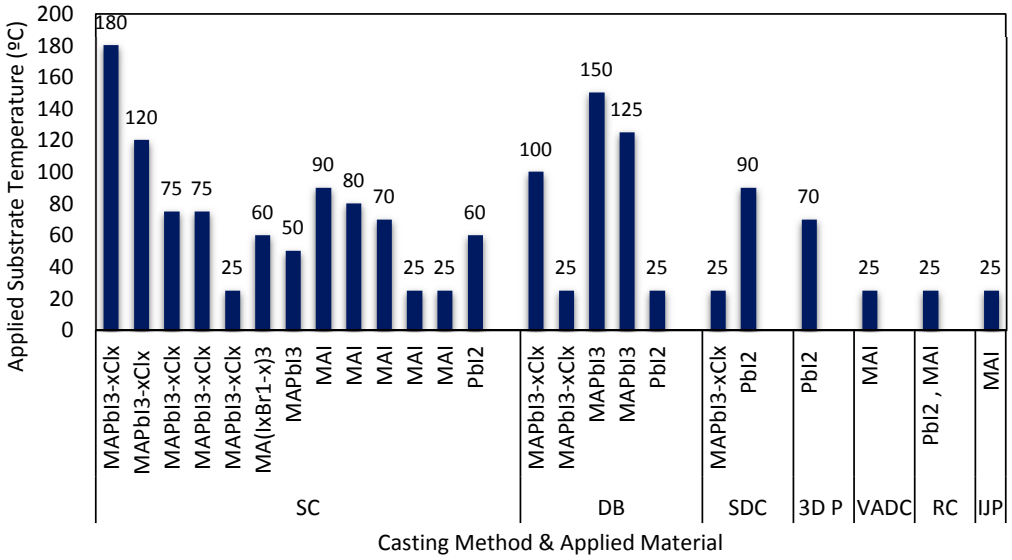

Figure 5. Employed substrte temeratures during the fabrication of perovsite films by various (large scale) techniques. (data taken from Refs. [3,7,8,13,16,18–22,24,25,30–37]). Abreviations: SC: Spray coating; DB: Doctor blading; SDC: Slot-die coating; 3D P: 3D printing based on SDC and N_2 gas-blowing; VADC: Vibration-assisted drop casting; RC: Roller coating; IJP: Inkjet printing.

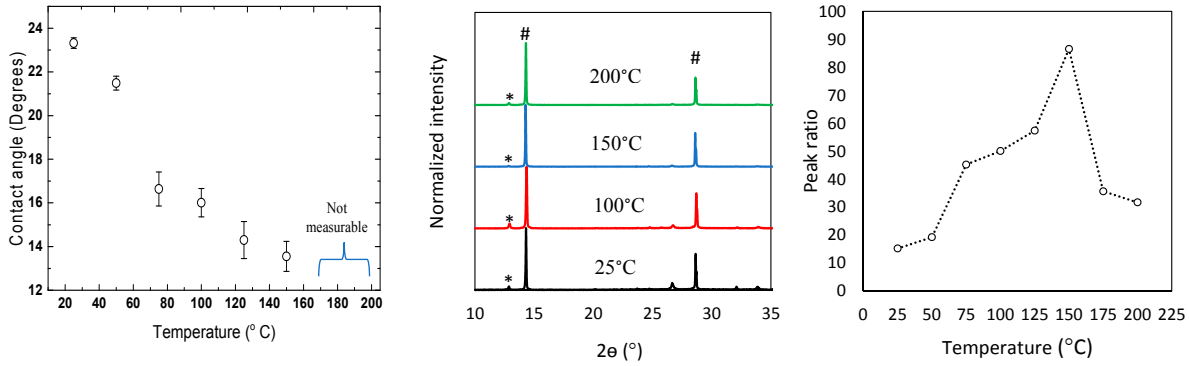

(**a**) (**b**) (**c**)

Figure 6. (**a**) contact angle of the perovskite solution droplets ($MAPbI_{3-x}Cl_x$ in DMF) versus substrate temperature; (**b**) XRD patterns of $MAPbI_{3-x}Cl_x$ perovskite films, spray deposited on FTO-coated glass substrates at various substrate temperatures (# and * represent the perovskite and PbI_2 peaks, respectively); (**c**) the quantified conversion ratios at various substrate temperatures. At temperatures higher than the boiling point of DMF (>153 °C), measurement of the contact angle was found to be not accurate, due to rapid solvent evaporation. It is noted that, after deposition, all perovskite films were annealed at 100 °C for 2 h.

The third and last parameter to optimize is the number of spray passes for the used spray nozzle and spray conditions (Table 1). The number of spray passes affects the film coverage, thickness, and roughness. In general, photons with long wavelengths are better absorbed in thicker films, which

could translate to a higher current density in the active layer [25]; however, enhanced absorption occurs at the cost of increased charge recombination and the loss of the current density [25]. The limitation of charge diffusion length in perovskite films also confines the admissible span of thicknesses. In $MAPbI_{3-x}Cl_x$ mixed halide perovskite, the charge diffusion length has been measured to be around 1000 nm, while, in $MAPbI_3$ single halide perovskite, it is near 100 nm [3]. Therefore, there is a specific range of thicknesses in which the highest current from a perovskite film could be extracted. In this work, adjusting the thickness was performed by using multiple spray passes. A single spray pass is the travelling of the spray nozzle arm over the substrate with a specific nozzle velocity. Multiple-pass spraying is comprised of several consecutive single spray passes back and forth in a predesigned raster pattern to improve the coverage and achieve a desired thickness. Figure 7 shows the measured thickness and roughness values of the perovskite films, sprayed using 40, 70, and 100 passes, on the substrates kept at the ambient temperature. Coverage measurements revealed that, at the used spray flow rate and spray nozzle speed (Table 1), spraying using 40 and 70 passes was not enough to cover the film completely. Raising the passes to 100 resulted in full coverage of the substrate. Obviously, the film thickness increases by raising the number of spray passes; however, the 40-pass-spray-on film showed the highest roughness, which is due to the excessive number of pinholes. However, in the two other cases, increasing the number of passes from 70 to 100, resulted in an increase in the roughness again (Figure 7b). This is in agreement with the result of other reports, which declared that the roughness of spray-on perovskite films increases by increasing the thickness [25]. It is noted that in less-crystalline or amorphous films, such as polymeric films, the correlation between the number of spray passes and roughness may be somewhat different from what was observed here for perovskite films, simply because, in polymeric films, the phenomenon of crystallization dewetting and the formation of large grains is absent or it is insignificant [40].

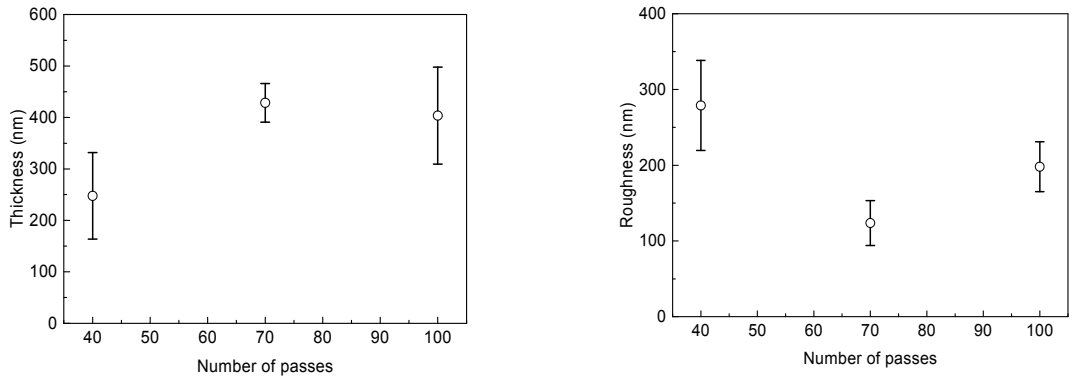

Figure 7. Measured (**a**) thickness and (**b**) roughness of spray-on perovskite films deposited on the substrates kept at the ambient temperature, at various number of spray passes.

To fabricate the best functional perovskite film, i.e., lowest roughness and proper thickness with negligible PbI_2 impurity, the spraying process was repeated using different passes (40, 70 and 100) on hotplates at the optimum temperature of 150 °C, which yields the best conversion ratio (Figure 8). Again, the full coverage is achieved at 100 passes, while the thickness and roughness decreased in all cases, compared with the samples fabricated on the substrates kept at the ambient temperature.

Figure 9 shows the SEM images of spray-on perovskite films deposited on the hotplates kept at 150 °C, while the number of passes varies. The average coverage, denoted as C on the images, obtained from the SEM images, reveals that a fully-covered film was obtained after 100 passes. The coverage was obtained by image processing using the ImageJ software (version 1.51j, National Institutes of Health (NIH), Bethesda, MD, USA).

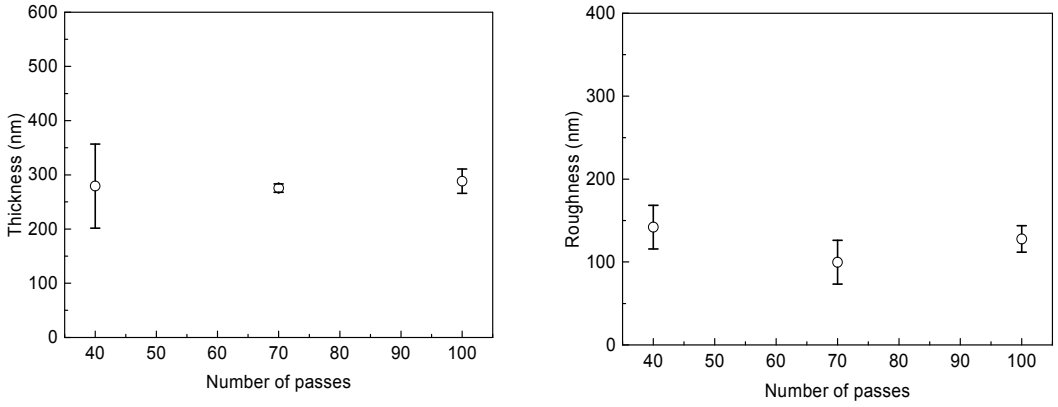

(**a**) (**b**)

Figure 8. Measured (**a**) thickness and (**b**) roughness of spray-on perovskite films deposited on the substrates kept at 150 °C, at various number of spray passes.

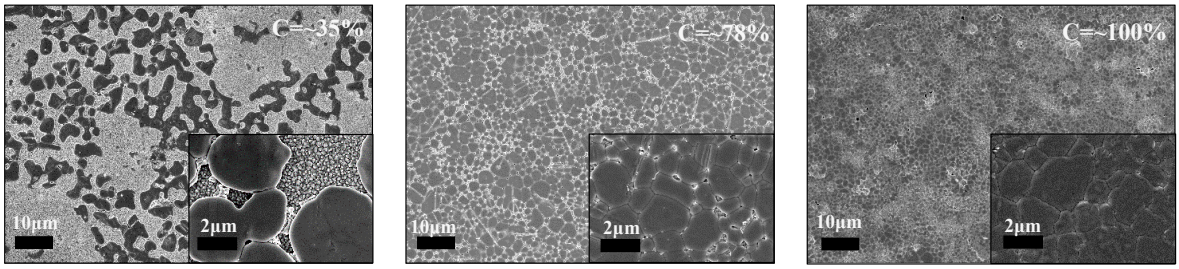

(**a**) (**b**) (**c**)

Figure 9. SEM images of spray-on perovskite films deposited on FTO-coated glass substrates at substrate temperatures of 150 °C. The number of spray passes are (**a**) 40; (**b**) 70; and (**c**) 100. Letter C refers to the percentage of coverage of perovskite layer on the substrates.

Interestingly, as depicted in Figure 10, the application of the high temperature substrate results in a decrease in the standard deviation of roughness and thickness data of spray-on films with respect to their counterparts fabricated at the ambient temperature. This is an important factor to increase the device reproducibility of large-area perovskite films. According to Figure 8a, the average thickness values of all three spray-on samples is less than 300 nm, which is acceptable for mixed halide perovskite films to perform well in a PSC [24]. In Figure 10, the spray-on films made using 70 passes show the minimum standard deviation in their thicknesses. The same films have the lowest roughness as well (Figure 8b). However, these films suffer from inadequate coverage (78%). Thus, the film made using 100 passes on the hotplate kept at 150 °C is considered as the best film.

The perovskite films, sprayed using 100 passes on the substrates kept at 25 and 150 °C, are compared using optical and SEM images shown in Figure 11a,b. The absorbance spectra of the same films are also shown in Figure 11c. According to the thickness values given in Figures 7a and 8a, the film sprayed using 100 passes on the substrate kept at the ambient temperature is thicker than the film sprayed on the hotplate at 150 °C, while its absorbance shown in Figure 11c is lower in a wide range of wavelengths. This may have originated from two sources. Firstly, high roughness in spray-on films may decrease the light absorbance [41]. Based on the roughness data of Figures 7b and 8b, the former film is rougher, i.e., its local variation of thickness is higher than the latter film. Inset optical images in Figure 11a,b also verify that the film fabricated on the hotplate is smoother than the film sprayed on the substrate kept at the ambient temperature, thus it can absorb the light more efficiently. Secondly, according to the conversion ratio data shown in Figure 6c, there is more

PbI_2 impurity in the perovskite film fabricated at 25 °C, with respect to the film deposited on the hotplate kept at 150 °C. Therefore, the film deposited on the hotplate is more functional and thus capable of better photon absorption, considering that the bandgap of the perovskite films is suitable for the absorption of photons in the visible range. Figure 11d is a picture of the fabricated film (5×5 cm^2), made using the optimum conditions of 100 spray passes deposited on the hotplate kept at 150 °C, using a perovskite solution concentration of 10 wt.%. The raster movement of the spray nozzle is also illustrated schematically on this picture. This spray-on film is semitransparent and thus has the capability to be used as a second absorber layer to make tandem perovskite–copper indium gallium diselenide (CIGS) or perovskite–silicon solar cells.

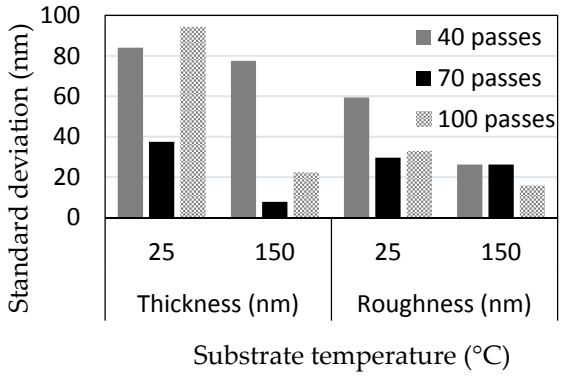

Figure 10. Standard deviation of the roughness and thickness data of perovskite films fabricated by various spray passes on the substrates kept at 25 and 150 °C. High substrate temperature improves reproducibility of the data.

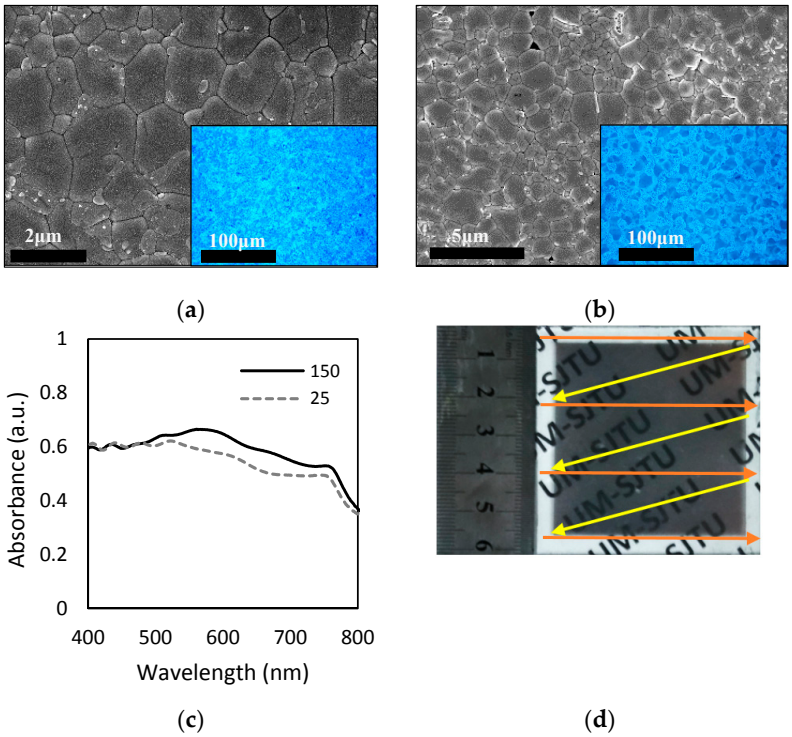

Figure 11. SEM and optical (inset) images of spray-on perovskite films made at substrate temperature of (**a**) 25 °C and (**b**) 150 °C. (**c**) absorbance spectra of perovskite films sprayed on FTO-coated glass kept at 150 °C; (**d**) the spray-on film deposited on the hotplate kept at 150 °C and the deposition pattern based on a zigzag movement of the spray nozzle over the substrate. The films were made at optimum condition of 100 spray passes using a 10 wt.% solution concentration.

4. Conclusions

A continuous, uniform, and pinhole-free perovskite thin film was fabricated by spray coating with an effective squared area of 25 cm^2. Optimum concentration of the mixed halide perovskite precursor (10 wt.% of $MAPbI_{3-x}Cl_x$ in DMF) and substrate temperature (150 °C) were determined as two essential parameters that strongly affect the morphology of the spray-on film. The optimum concentration and substrate temperature may be generalized to other spray systems. Then, for the spray nozzle used in this study, for the given spray flow rate and nozzle speed, the number of spray passes was optimized (100 spray passes). The combination of the best solution concentration, substrate temperature, and the number of spray passes produced a fully functional perovskite film with high surface area suitable for the commercialization of the technology. We also measured the contact angle, surface tension, and viscosity of the mixed halide perovskite solution in different concentrations, in order to find the optimum range of concentration. In order to choose the best substrate temperature, at first, we measured the contact angle of perovskite droplets on the hotplates at various temperatures. It was observed that a higher substrate temperature leads to a higher surface wettability (lower contact angle). At 150 °C, which is around the boiling point of DMF, we also observed the highest conversion ratio (efficient conversion of perovskite precursors to perovskite), which is a measure of the percentage of PbI_2 impurity in the perovskite film. Spraying of 10 wt.% mixed halide perovskite using 100 passes on a hotplate kept at 150 °C resulted in a fully-covered film with the lowest thickness and roughness, compared to the films made on the substrates kept at room temperature. Standard deviation of the thickness and roughness of the films made on hot substrates also decreased, which is an indication of increased reproducibility of the process. Although the fabricated large-area perovskite films demonstrated superior morphological and optoelectronic functionality, it is noted that their photovoltaic performance would be determined when used in a complete device. The fabrication of such large area devices is challenging and entails the optimization of all layers, which was beyond the scope of this work.

Acknowledgments: Research funding from the Shanghai Municipal Education Commission in the framework of the Oriental scholar and distinguished professor designation and funding from the National Natural Science Foundation of China (NSFC) is acknowledged.

Author Contributions: Mehran Habibi and Morteza Eslamian conceived the work; Mehran Habibi designed and performed the experiments regarding the optimization of perovskite layers, conducted characterization tests, and discussed the results. Amin Rahimzadeh performed the tests concerning the physical properties of perovskite solutions and interpreted the results. Inas Bennouna assisted with the experiments and characterizations; and Mehran Habibi, Amin Rahimzadeh and Morteza Eslamian wrote the paper. All authors read and approved the paper.

Conflicts of Interest: The authors declare no conflict of interest.

References

1. Efficiency chart. Available online: http://www.nrel.gov/pv/assets/images/efficiency_chart.jpg (accessed on 10 March 2017).
2. Habibi, M.; Rahimzadeh, A.; Eslamian, M. On dewetting of thin films due to crystallization (crystallization dewetting). *Eur. Phys. J. E Soft Matter.* **2016**, *39*, 30. [CrossRef] [PubMed]
3. Habibi, M.; Zabihi, F.; Ahmadian-Yazdi, M.R.; Eslamian, M. Progress in emerging solution-processed thin film solar cells–Part II: Perovskite solar cells. *Renew. Sustain. Energy Rev.* **2016**, *62*, 1012–1031. [CrossRef]
4. Cai, B.; Zhang, W.-H.; Qiu, J. Solvent engineering of spin-coating solutions for planar-structured high-efficiency perovskite solar cells. *Chin. J. Catal.* **2015**, *36*, 1183–1190. [CrossRef]
5. Jeon, N.J.; Noh, J.H.; Kim, Y.C.; Yang, W.S.; Ryu, S.; Seok, S.I. Solvent engineering for high-performance inorganic-organic hybrid perovskite solar cells. *Nat. Mater.* **2014**, *13*, 897–903. [CrossRef] [PubMed]
6. Ahmadian-Yazdi, M.; Zabihi, F.; Habibi, M.; Eslamian, M. Effects of Process Parameters on the Characteristics of Mixed-Halide Perovskite Solar Cells Fabricated by One-Step and Two-Step Sequential Coating. *Nanoscale Res. Lett.* **2016**, *11*, 408. [CrossRef] [PubMed]

7. Ramesh, M.; Boopathi, K.M.; Huang, T.Y.; Huang, Y.C.; Tsao, C.S.; Chu, C.W. Using an airbrush pen for layer-by-layer growth of continuous perovskite thin films for hybrid solar cells. *ACS Appl. Mater. Interfaces* **2015**, *7*, 2359–2366. [CrossRef] [PubMed]
8. Mohammadian, N.; Alizadeh, A.H.; Moshaii, A.; Gharibzadeh, S.; Alizadeh, A.; Mohammadpour, R.; Fathi, D. A two-step spin-spray deposition processing route for production of halide perovskite solar cell. *Thin Solid Films* **2016**, *616*, 754–759. [CrossRef]
9. Gong, X.; Li, M.; Shi, X.-B.; Ma, H.; Wang, Z.-K.; Liao, L.-S. Controllable Perovskite Crystallization by Water Additive for High-Performance Solar Cells. *Adv. Funct. Mater.* **2015**, *25*, 6671–6678. [CrossRef]
10. Liang, P.W.; Liao, C.Y.; Chueh, C.C.; Zuo, F.; Williams, S.T.; Xin, X.K.; Lin, J.; Jen, A.K. Additive enhanced crystallization of solution-processed perovskite for highly efficient planar-heterojunction solar cells. *Adv. Mater.* **2014**, *26*, 3748–3754. [CrossRef] [PubMed]
11. Lau, C.F.J.; Deng, X.; Ma, Q.; Zheng, J.; Yun, J.S.; Green, M.A.; Huang, S.; Ho-Baillie, A.W.Y. $CsPbIBr_2$Perovskite Solar Cell by Spray-Assisted Deposition. *ACS Energy Lett.* **2016**, *1*, 573–577. [CrossRef]
12. Razza, S.; Di Giacomo, F.; Matteocci, F.; Cinà, L.; Palma, A.L.; Casaluci, S.; Cameron, P.; D'Epifanio, A.; Licoccia, S.; Reale, A.; et al. Perovskite solar cells and large area modules (100 cm^2) based on an air flow-assisted PbI_2 blade coating deposition process. *J. Power Sources* **2015**, *277*, 286–291. [CrossRef]
13. Yeo, J.-S.; Lee, C.-H.; Jang, D.; Lee, S.; Jo, S.M.; Joh, H.-I.; Kim, D.-Y. Reduced graphene oxide-assisted crystallization of perovskite via solution-process for efficient and stable planar solar cells with module-scales. *Nano Energy* **2016**, *30*, 667–676. [CrossRef]
14. Tait, J.G.; Manghooli, S.; Qiu, W.; Rakocevic, L.; Kootstra, L.; Jaysankar, M.; Masse de la Huerta, C.A.; Paetzold, U.W.; Gehlhaar, R.; Cheyns, D.; et al. Rapid composition screening for perovskite photovoltaics via concurrently pumped ultrasonic spray coating. *J. Mater. Chem. A* **2016**, *4*, 3792–3797. [CrossRef]
15. Markus, H.; Henrik, F.D.; Krebs, F.C. Development of Lab-to-Fab Production Equipment Across Several Length Scales for Printed Energy Technologies, Including Solar Cells. *Energy Technol.* **2015**, *3*, 293–304.
16. Huang, H.; Shi, J.; Zhu, L.; Li, D.; Luo, Y.; Meng, Q. Two-step ultrasonic spray deposition of $CH_3NH_3PbI_3$ for efficient and large-area perovskite solar cell. *Nano Energy* **2016**, *27*, 352–358. [CrossRef]
17. Eslamian, M. Spray-on thin film PV solar cells: Advances, potentials and challenges. *Coatings* **2014**, *4*, 60–84. [CrossRef]
18. Chandrasekhar, P.S.; Kumar, N.; Swami, S.K.; Dutta, V.; Komarala, V.K. Fabrication of perovskite films using an electrostatic assisted spray technique: the effect of the electric field on morphology, crystallinity and solar cell performance. *Nanoscale* **2016**, *8*, 6792–6800. [CrossRef] [PubMed]
19. Heo, J.H.; Lee, M.H.; Jang, M.H.; Im, S.H. Highly efficient CH3NH3PbI$_{3-x}$Cl$_x$ mixed halide perovskite solar cells prepared by re-dissolution and crystal grain growth via spray coating. *J. Mater. Chem. A* **2016**, *4*, 17636–17642. [CrossRef]
20. Abdollahi, N.B.; Gharibzadeh, S.; Ahmadi, V.; Shahverdi, H.R. New Scalable Cold-Roll Pressing for Post-treatment of Perovskite Microstructure in Perovskite Solar Cells. *J. Phys. Chem. C* **2016**, *120*, 2520–2528. [CrossRef]
21. Jung, Y.S.; Hwang, K.; Scholes, F.H.; Watkins, S.E.; Kim, D.Y.; Vak, D. Differentially pumped spray deposition as a rapid screening tool for organic and perovskite solar cells. *Sci. Rep.* **2016**, *6*, 20357. [CrossRef] [PubMed]
22. Zabihi, F.; Ahmadian-Yazdi, M.R.; Eslamian, M. Fundamental Study on the Fabrication of Inverted Planar Perovskite Solar Cells Using Two-Step Sequential Substrate Vibration-Assisted Spray Coating (2S-SVASC). *Nanoscale Res. Lett.* **2016**, *11*, 71. [CrossRef] [PubMed]
23. Habibi, M.; Ahmadian-Yazdi, M.R.; Eslamian, M. Optimization of spray coating for the fabrication of planar perovskite solar cells. *At. Sprays* **2017**. under review.
24. Barrows, A.T.; Pearson, A.J.; Kwak, C.K.; Dunbar, A.D.F.; Buckley, A.R.; Lidzey, D.G. Efficient planar heterojunction mixed-halide perovskite solar cells deposited via spray-deposition. *Energy Environ. Sci.* **2014**, *7*, 2944. [CrossRef]
25. Das, S.; Yang, B.; Gu, G.; Joshi, P.C.; Ivanov, I.N.; Rouleau, C.M.; Aytug, T.; Geohegan, D.B.; Xiao, K. High-Performance Flexible Perovskite Solar Cells by Using a Combination of Ultrasonic Spray-Coating and Low Thermal Budget Photonic Curing. *ACS Photonics* **2015**, *2*, 680–686. [CrossRef]
26. Mullins, W.W.; Sekerka, R.F. Morphological Stability of a Particle Growing by Diffusion or Heat Flow. *J. Appl. Phys.* **1963**, *34*, 323–329. [CrossRef]

27. Sear, R.P. Nucleation at contact lines where fluid–fluid interfaces meet solid surfaces. *J. Phys. Condens. Matter.* **2007**, *19*, 466106. [CrossRef]
28. Djikaev, Y.S.; Ruckenstein, E. Thermodynamics of Heterogeneous Crystal Nucleation in Contact and Immersion Modes. *J. Phys. Chem. A* **2008**, *112*, 11677–11687. [CrossRef] [PubMed]
29. Rahimzadeh, A.; Eslamian, M. Stability of thin liquid films subjected to ultrasonic vibration and characteristics of the resulting thin solid films. *Chem. Eng. Sci.* **2017**, *158*, 587–598. [CrossRef]
30. Deng, Y.; Peng, E.; Shao, Y.; Xiao, Z.; Dong, Q.; Huang, J. Scalable fabrication of efficient organolead trihalide perovskite solar cells with doctor-bladed active layers. *Energy Environ. Sci.* **2015**, *8*, 1544–1550. [CrossRef]
31. Wei, Z.; Chen, H.; Yan, K.; Yang, S. Inkjet printing and instant chemical transformation of a CH3NH3PbI3/nanocarbon electrode and interface for planar perovskite solar cells. *Angew. Chem.* **2014**, *53*, 13239–13243. [CrossRef] [PubMed]
32. Hwang, K.; Jung, Y.S.; Heo, Y.J.; Scholes, F.H.; Watkins, S.E.; Subbiah, J.; Jones, D.J.; Kim, D.Y.; Vak, D. Toward large scale roll-to-roll production of fully printed perovskite solar cells. *Adv. Mater.* **2015**, *27*, 1241–1247. [CrossRef] [PubMed]
33. Schmidt, T.M.; Larsen-Olsen, T.T.; Carlé, J.E.; Angmo, D.; Krebs, F.C. Upscaling of Perovskite Solar Cells: Fully Ambient Roll Processing of Flexible Perovskite Solar Cells with Printed Back Electrodes. *Adv. Energy Mater.* **2015**, *5*, 69. [CrossRef]
34. Kim, J.H.; Williams, S.T.; Cho, N.; Chueh, C.-C.; Jen, A.K.Y. Enhanced Environmental Stability of Planar Heterojunction Perovskite Solar Cells Based on Blade-Coating. *Adv. Energy Mater.* **2015**, *5*, 1401229. [CrossRef]
35. Back, H.; Kim, J.; Kim, G.; Kyun, K.T.; Kang, H.; Kong, J.; Lee, H.S.; Lee, K. Interfacial modification of hole transport layers for efficient large-area perovskite solar cells achieved via blade-coating. *Sol. Energy Mater. Sol. Cells* **2016**, *144*, 309–315. [CrossRef]
36. Park, S.-M.; Noh, Y.-J.; Jin, S.-H.; Na, S.-I. Efficient planar heterojunction perovskite solar cells fabricated via roller-coating. *Solar Energy Mater. Solar Cells* **2016**, *155*, 14–19. [CrossRef]
37. Mallajosyula, A.T.; Fernando, K.; Bhatt, S.; Singh, A.; Alphenaar, B.W.; Blancon, J.-C.; Nie, W.; Gupta, G.; Mohite, A.D. Large-area hysteresis-free perovskite solar cells via temperature controlled doctor blading under ambient environment. *Appl. Mater. Today* **2016**, *3*, 96–102. [CrossRef]
38. Dualeh, A.; Gao, P.; Seok, S.I.; Nazeeruddin, M.K.; Grätzel, M. Thermal behavior of methylammonium lead-trihalide perovskite photovoltaic light harvesters. *Chem. Mater.* **2014**, *26*, 6160–6164. [CrossRef]
39. Brunetti, B.; Cavallo, C.; Ciccioli, A.; Gigli, G.; Latini, A. On the thermal and thermodynamic (in)stability of methylammonium lead halide perovskites. *Sci. Rep.* **2016**, *6*, 31896. [CrossRef] [PubMed]
40. Xie, Y.; Gao, S.; Eslamian, M. Fundamental study on the effect of spray parameters on characteristics of P3HT:PCBM active layers made by spray coating. *Coatings* **2015**, *5*, 488–510. [CrossRef]
41. Wengeler, L.; Schmitt, M.; Peters, K.; Scharfer, P.; Schabel, W. Comparison of large scale coating techniques for organic and hybrid films in polymer based solar cells. *Chem. Eng. Process. Process Intensif.* **2013**, *68*, 38–44. [CrossRef]